

Diagnostic Value of the Post-Processing Technique of Multi-Slice Spiral CT in Orbital Cyst Diseases

Liang Li¹, Jinfa Liang², Rongzhen Liang¹, Bingtian Zeng¹

¹ Shiqi People's Hospital of Panyu District, Guangzhou 511450, China

² Guangzhou Panyu Central Hospital, Guangzhou 511400, China

Abstract

Purpose: To analyze the features of CT imaging of orbital cystic disease.

Methods: A total of 30 patients were pathologically confirmed with orbital cystic disease between January 2007 and March 2012. Prior to operation, the participants underwent CT scans with image processing by maximum intensity projection (MIP) and volume rendering (VR). Preoperative CT diagnostic outcomes were compared with postoperative pathological findings.

Results: The patients presented with round, oval and dumb-bell shaped masses. Fourteen cases of dermoid cyst and 8 cases of epidermoid cyst showed heterogeneous density. Among the dermoid cyst patients, 6 cases had demixing phenomenon, 3 cases had lipid drift and 5 cases showed mild or moderate intensity enhancement in the cyst wall. No intensity enhancement was observed in the epidermoid cyst patients. Five cases had high intensity due to hemorrhage and 3 patients presented with adjacent sclerotic arc compression; 5 cases of myxoid cyst had homogenous density and no intensity enhancement was found when iohexol was injected. Three patients with atheromatous cyst had heterogeneous density, with CT value ranging from -36Hu to 191Hu. Floss was noted centrally in 1 case and mild to moderate intensity enhancement was observed in the cyst wall with iohexol injection.

Conclusion: Multi-slice CT is useful in the diagnosis of orbital cystic disease. Multi-slice CT combined with image processing can be helpful in displaying the location and size of masses, and revealing the relationship between masses and surrounding bony tissue, providing an objective basis for surgical planning when combined with 3D-CT imaging. (*Eye Science* 2012; 27:89-93)

Keywords: CT; 3D imaging; eye; cyst

Orbital cyst diseases account for approximately 9% to 12% of all orbital tumorous lesions¹.

Proper preoperative determination of the nature and location of cysts contributes to the success of treatment regarding the imaging features of orbital masses. Due to sophisticated orbital structures and many vital and tiny tissues arranged in disorder, the explicit diagnosis of orbital diseases is extremely challenging. Preoperative misdiagnosis frequently occurs clinically, and incomplete therapy even leads to recurrence and fistulization. Imaging examination, as a noninvasive detection tool, not only determines the nature and location of orbital cyst lesions, but also provides evidence for clinical treatment and surgical design. At present, few studies have reported the misdiagnosis of orbital cyst diseases by using CT scans both domestically and internationally. The present study offers a retrospective analysis of the clinical information and CT scan images from 30 patients with orbital cyst diseases to deepen the understanding of CT imaging features. In addition, the authors also investigated the diagnostic values of multi-slice CT 3D reconstruction in determining the nature and location of orbital cyst lesions, aiming to improve the necessity and accuracy of CT scans.

Materials and methods

Clinical information

Thirty patients with orbital cyst diseases admitted to Shiqi People's Hospital of Panyu District (Guangzhou, China) between January 2007 and March 2012 were enrolled in this clinical trial (23 males, 7 females, aged between 3 and 47 years, 24.5 years on average, with a medical history ranging from 1 and 30 years). Clinical manifestations mainly included monocular or binocular orbital masses. Twelve patients had progressive exophthalmos without apparent discomforts or any changes in

skin color. Two patients with dermoid cyst (located between orbit and ethmoid sinus) presented with poor movement of masses and significant exophthalmos. The remaining cases had relatively normal mass movement (located at deep orbit) without any clinical manifestations, which were diagnosed accidentally during physical tests.

CT scans

CT scanning

Philips Brilliance 16-slice spiral CT scanner, MedRad double tubes syringe, and nonionic contrast agent iohexol (300 mgI/ml) were used. All patients underwent routine orbital CT plain scan, at horizontal axis position, OML as scan baseline, scanning range upper and lower orbital walls. Eighteen patients received enhanced CT scan. Scan parameters: tube voltage 120 kV, tube current 250 mAs, slice thickness 0.8 mm, 0.4 mm interval, and pitch 3 mm.

Post-processing reconstruction

The original images were reconstructed with a minimal slice thickness of 0.8 mm and interval of 0.4 mm, and then transferred to the Extended Brilliance TM Workspace (Release 3.0.1.3200) workstation. All the images were processed by maximum intensity projection (MIP) and volume rendering (VR). The original and processed images were evaluated by two experienced physicians from imaging department regarding the capability of MIP and VR for displaying orbital cyst lesions.

Operation and pathological examinations

Pathological test results confirmed 14 cases of dermoid cyst, eight cases of epidermoid cyst, five cases of mucous cyst, and three cases of sebaceous cyst. Twenty-eight patients underwent tumor resection at one week and two months after CT scans, and two patients had puncture biopsy. The resected and puncture tissues were further diagnosed by HE staining and immunochemical analysis.

Results

Location and morphology of orbital cysts

Dermoid cysts ($n=14$) and epidermoid cysts ($n=8$) occurred in inner and outer orbital walls, zygomatic-forehead suture, into muscle cone and beneath eyelid skin, and showed round and oval shape. The

dermoid cyst in dumbbell shape, located at right nasal bone, grew along the bone suture and crossed the orbital wall (Figure 1). Mucous cysts ($n=5$) were mainly distributed within orbit, outer and upper walls, and generally in an oval shape. Sebaceous cysts were detected beneath eyelid skin, and most cysts showed oval or round-like shape.

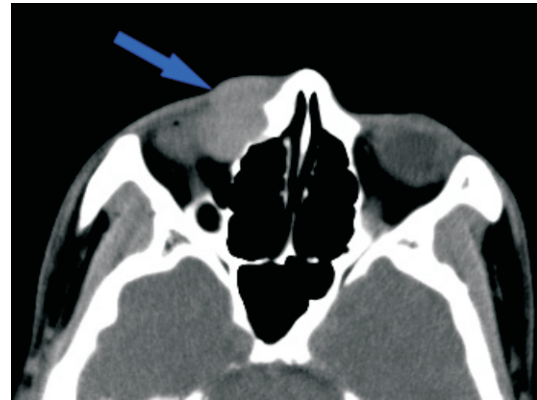


Figure 1 Dermoid cysts, in dumbbell shape, grew along bone suture on the right side of nasal

Density of cysts

Dermoid cysts ($n=14$) and epidermoid cysts ($n=8$) had heterogeneous density, CT value 0 Hu to 180 Hu. Six cases with dermoid cysts had demixing phenomenon, three cases had lipid drifts, and five cases showed mild or moderate intensity enhancement in cyst walls; cyst wall thickness ranged from 0.6 to 1.5 mm (Figure 2). No enhancement was observed in epidermoid cyst wall. Five cases had high intensity due to hemorrhage, and five patients with mucous cysts had homogeneous density and no enhancement noted when iohexol was injected. Three cases with dermoid cysts had heterogenous density, with CT value of -36 Hu to 110 Hu. Floss was found in the central mass in one patient. Enhanced CT scan showed mild and moderate enhancement in patients with intact cyst wall. Two patients did not show apparent cyst wall.

Relationship between cysts and surrounding bone tissues

Obvious compressive orbital deformation and orbital depression were observed in patients with dermoid cysts ($n=10$) and epidermoid cysts ($n=6$) (Figures 3,4). Bone destruction and defect changes were noted in two patients with dermoid cysts. Dermoid

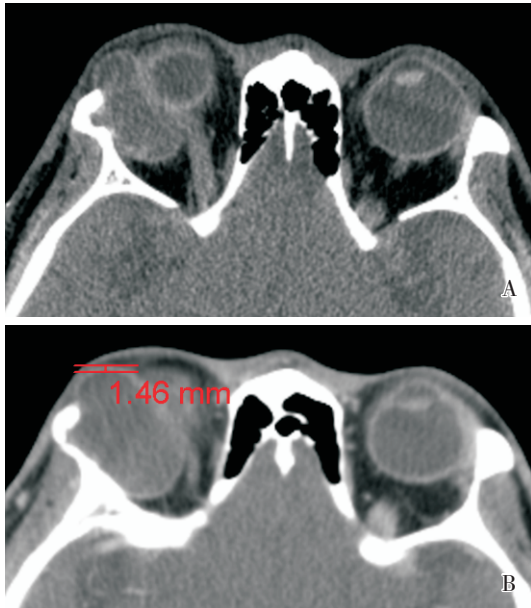


Figure 2 Mild intensity enhancement was noted in the cystic wall of dermoid cyst on the right side of nasal bone, cystic wall 1.46 mm in thickness. A: orbital axis plain scan; B: orbital axis enhanced scan

cysts ($n=2$) and epidermoid cysts ($n=2$) were found within muscle cone. Sebaceous cysts ($n=3$) were located at subconjunctival palpebrae, distant from sclerotic, and no sign of sclerotic changes was found. The size of mucous cysts was not large, and no significant compressive orbital changes were observed.

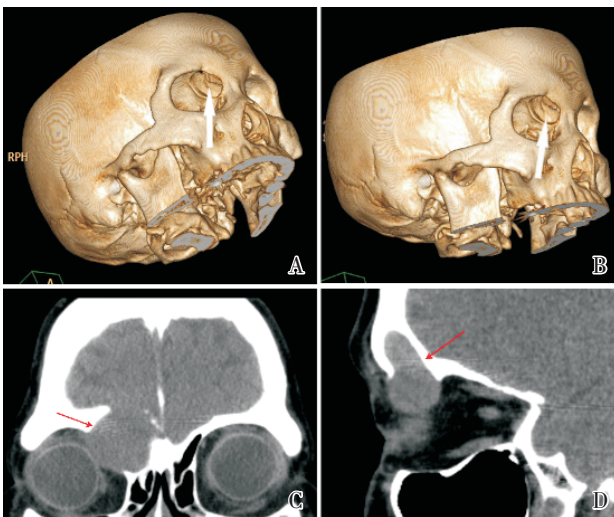


Figure 3 VR images (A and B) clearly show the compression status of interior wall of the right orbit. Plain scan sagittal plane (C) and coronal plane (D) were in agreement with VR images.

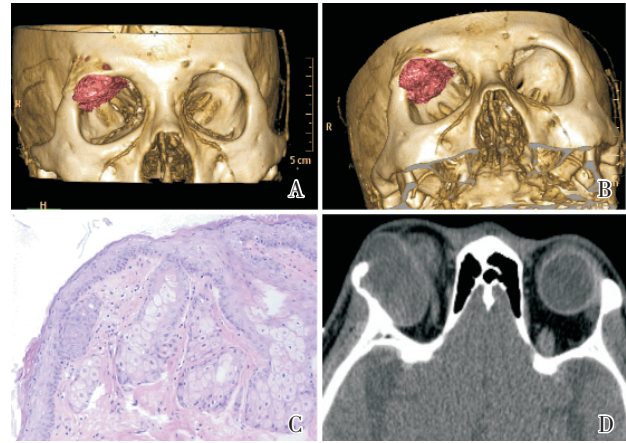


Figure 4 VR images (A and B) show regular mass shape and no sign of compression-induced sclerotic changes; the lesions were characterized as oval masses with clear boundary extra conal orbit, to be considered as benign dermoid cyst (C), consistent with pathological results (D).

Surgical outcomes

For the 30 patients with orbital cyst lesions, HR-CT scan and postoperative pathological examination yielded basically consistent outcomes (Figure 4). High-resolution CT scans revealed 13 cases of dermoid cysts, 7 cases of epidermoid cysts, 5 cases of mucous cysts, and 3 cases of sebaceous cysts. Post-processing technique combined with CT observations at horizontal axis position gained a high accuracy of displaying orbital cyst lesions.

Discussion

Along with the advancement of imaging instruments, image processing techniques and image digital modeling, a noninvasive detection tool of ocular ultrastructure has caught more and more attention. CT scanning, as a 3D imaging technique, can display the lesion characteristics by continuously collecting traverse imaging information and create stereo images by 3D reconstruction method².

MIP and VR are most commonly utilized when performing 16-slice spiral CT scan and post-processing technique. VR imaging can configure CT values into different degrees of transparency. It utilizes virtual lighting effect to reveal 3D structures by using various pseudo colors and gray scales. The post-processing procedure is relatively easy, and the 3D images can be automatically generated by software.

MIP reconstruction can selectively reconstruct images from multiple centers, remove the interference from images outside the observation area, and is easy to perform. Compared with VR, MIP has advantages in the diagnosis of lung, nervous, middle ear, and bone trabecular lesions³⁻⁶.

Orbital cysts are divided into epithelial cell-derived and non-epithelial cyst-derived cysts. Epithelial cell-derived cyst lesions mainly include dermoid cysts, epidermoid cysts, sebaceous cysts, mucous cysts, etc. Non-epithelial cell-derived cysts mainly consist of blood, nerve-derived and infective cysts, etc⁷⁻⁸. In clinical settings, dermoid cyst and epidermoid cysts account for approximately 3 to 9% of orbital tumorous lesions⁹⁻¹⁰. In current study, the imaging features of epithelial cell-derived cysts were the main focus. In addition, the sites of orbital cyst lesions exert certain effects upon clinical diagnosis. It has been generally considered that the lesions located at orbital surface are easily diagnosed due to the apparent symptoms, whereas those cysts at deep orbit are difficult to detect because of insignificant clinical manifestations. In this case, preliminary diagnosis can be made according to imaging characteristics¹¹.

Few studies have reported CT manifestations and the application of post-processing technique in the diagnosis of orbital cysts. CT scans showed that the 30 patients presented with round and oval cysts, and the masses grew expansively with clear boundaries. Most dermoid cysts and epidermoid cysts had a heterogeneous density, and low-density lipid was noted in dermoid cyst patients, demixing phenomenon and high-density calcification plaque in some cases. Mild and moderate intensity was found in cyst walls when iohexol was injected, with cyst wall thicknesses of 0.6 to 1.0 mm, which were basically consistent with the findings of previous studies¹². Epidermoid cysts were mainly in round shapes with clear boundaries. No abnormal low-intensity image was seen due to abundant cholesterol crystal within orbital cysts, similar to the findings by Nagasawa, in which flake high-intensity image was observed in the center of partial tumors probably caused by internal hemorrhage¹³. Mucous cysts showed homogeneous density, and no enhancement was noted when iohexol was injected. CT scans revealed heterogeneous density in

sebaceous cysts (CT value -36 Hu to 110 Hu). Floss could be observed in the center of some lesions with intact or defected cyst walls. Mild and moderate intensity was observed in patients with intact cyst walls.

CT scans combined with post-processing technique can display the relationship between orbital cyst lesions and surrounding tissues. Although contrast agents gain certain advantages regarding determining the nature of cysts, the imaging tool alone has limitations in the diagnosis of orbital cysts. It is difficult to distinguish dermoid cysts from epidermoid cysts and dysembryoma. However, the three types of cysts differ in terms of histoembryology, site of onset, patients' age, and imaging features. Dermoid cysts frequently occur near eyeballs, grow along bone suture, and adhere to periosteum. Dermoid cysts have intact envelope, and significant enhancement was observed in cyst walls containing a substantial amount of glial fiber. Epidermoid cysts mainly attack surrounding eyelids at a relatively younger age. A teratoma is an encapsulated tumor with tissue or organ components resembling normal derivatives of all three germ layers¹⁴. The authors consider that preoperative missed diagnosis mainly contributes to poor understanding of discriminating three types of cysts. Besides, it is necessary to identify lymphoma from dermoid cysts and epidermoid cysts. Lymphoma frequently occurs within muscle cone, always accompanied by hemorrhage. The density varies according to different stages. A slight amount of calcification can be found. Lymphoma has insignificant compression upon adjacent sclerotin.

Therefore, processing technique in post multi-slice spiral CT scanning has certain diagnostic values in determining the nature and location of orbital cyst lesions.

References

- 1 Henderson JW. Orbital tumors. Third Ed. New York: Raven Press Ltd. 1994; 53-88.
- 2 Guyomarc'h P, Dutailly B, Couture C, et al. Anatomical placement of the human eyeball in the orbit-validation using CT scans of living adults and prediction for facial approximation. *Forensic Sci.* 2012 Mar 5. [Epub ahead of print]
- 3 Ichikado K, Muranaka H, Gushima Y, et al. Fibroprolifer-

- ative changes on high-resolution CT in the acute respiratory distress syndrome predict mortality and ventilator dependency: a prospective observational cohort study. *BMJ Open*.2012 Mar 1;2(2): e000545.
- 4 Burghardt AJ, Link TM, Majumdar S, et al. High-resolution Computed Tomography for Clinical Imaging of Bone Microarchitecture. *Clin Orthop Relat Res*.2011 Aug;469(8):2179–2193.
 - 5 Yu Z, Wang Z, Yang B, et al. The value of preoperative CT scan of tympanic facial nerve canal in tympanomastoid surgery. *Acta Otolaryngol*.2011 Jul;131 (7):774–778.
 - 6 Sethom A, Akkari K, Dridi I, et al. Preoperative CT Scan in middle ear cholesteatoma. *Tunis Med*.2011 Mar;89(3):248–253.
 - 7 Rootman J. Structural lesions. In: Rootman J. *Diseases of the orbit, a multidisciplinary approach*. Philadelphia: Lippincott Williams & Wilkins, 2003; 417–434.
 - 8 Shields JA, Shields CL. Orbital cysts of childhood—classification clinical features and management. *Surv Ophthalmol*, 2004; 49(3):281–299.
 - 9 Nugent RA, Lapointe JS, Rootman J, et al. Orbital dermoids: features on CT. *Radiology*, 1987 Nov; 165(2): 475–478.
 - 10 Ahuja R, Azar NF. Orbital dermoids in children. *Semin Ophthalmol*, 2006 Jul–Sep; 21(3): 207–211.
 - 11 Onuigbo WI, Ezegwui IR. Ophthalmic presentation of epidermoid cysts in an African community. *Int Ophthalmol*, 2001; 24(5): 279–281.
 - 12 Chung EM, Murphey MD, Specht CS, et al. From the archives of the AFIP. Pediatric orbit tumors and tumorlike lesions: osseous lesions of the orbit. *Radiographics*, 2008; 28(4): 1193–1214.
 - 13 Nagasawa D, Yew A, Safae M, et al. Clinical characteristics and diagnostic imaging of epidermoid tumors. *Clin Neurosci*, 2011 Sep; 18(9): 1158–1162.
 - 14 Onuigbo WI, Ezegwui IR. Ophthalmic presentation of epidermoid cysts in an African community. *Int Ophthalmol*, 2001; 24(5): 279–281.